NANO LETTERS

Letter

pubs.acs.org/NanoLett

Auger Recombination in Self-Assembled Quantum Dots: Quenching and Broadening of the Charged Exciton Transition

Annika Kurzmann,*[,†] Arne Ludwig,[‡] Andreas D. Wieck,[‡] Axel Lorke,[†] and Martin Geller[†]

[†]Fakultät für Physik and CENIDE, Universität Duisburg-Essen, Lotharstraße 1, 47048 Duisburg, Germany

[‡]Chair of Applied Solid State Physics, Ruhr-Universität Bochum, Universitätsstr. 150, 44780 Bochum, Germany

Supporting Information

ABSTRACT: In quantum dots (QDs), the Auger recombination is a nonradiative process in which the electron−hole recombination energy is transferred to an additional carrier. It has been studied mostly in colloidal QDs, where the Auger recombination time is in the picosecond range and efficiently quenches the light emission. In self-assembled QDs, on the other hand, the influence of Auger recombination on the optical properties is in general neglected, assuming that it is masked by other processes such as spin and charge fluctuations. Here, we use time-resolved resonance fluorescence to analyze the Auger recombination and its influence on the optical properties of a single self-assembled QD. From excitation-power-dependent measurements, we find a long Auger recombination time of about 500 ns and a quenching of the trion transition by about 80%. Furthermore, we observe a broadening of the trion transition line width by up to a factor of 2. With a model based on rate equations, we are able to identify the interplay between tunneling and Auger rate as the underlying mechanism for the reduced intensity and the broadening of the line width. This demonstrates that self-assembled QDs can serve as an ideal model system to study how the charge recapture process, given by the band-structure surrounding the confined carriers, influences the Auger process. Our findings are not only relevant for improving the emission properties of colloidal QD-based emitters and dyes, which have recently entered the consumer market, but also of interest for more visionary applications, such as quantum information technologies, based on self-assembled quantum dots.

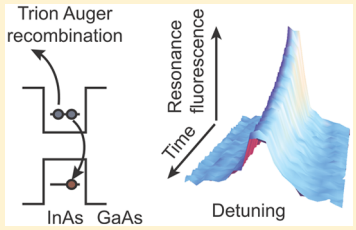

KEYWORDS: *Quantum dot, resonance fluorescence, Auger recombination, line width, trion*

The optical properties of solid-state quantum systems, such as self-assembled[1] or colloidal quantum dots (QDs),[2] are strongly influenced, and sometimes limited, by electron and hole interactions. Charge carriers in the vicinity of a dot lead to spectral broadening.[3−5] Furthermore, electron and hole interaction inside the dot enables Auger recombination, a nonradiative process, where the electron−hole recombination energy is transferred to an additional charge carrier.[6,7] The Auger process has been studied extensively in colloidal QDs,[8−10] where a fast Auger recombination time in the range below 1 ns[6,11] quenches the radiative recombination. This quenching limits the efficiency of optically active materials and devices based on colloidal QDs, such as light-emitting diodes[12,13] or single-photon sources.[14−16] The roles of both extrinsic effects (e.g., coupling to external carrier systems) and intrinsic processes (such as Auger recombination) are presently topics under intensive investigation.[17−19]

The Auger recombination time in self-assembled QDs can be extrapolated to be in the nano- to microsecond range,[20] orders of magnitude longer than for colloidal dots, so that this nonradiative process is of much lesser importance. Moreover, because of the highly ordered crystalline environment of self-assembled QDs, charging of nearby defects is strongly suppressed. This results in high quantum efficiency,[21] almost transform-limited single photons,[22−24] and a high photon indistinguishability.[25,26]

Here, we use an electrically controllable self-assembled QD as a model system to study the competition between Auger recombination (intrinsic) and coupling to an external charge reservoir (extrinsic). We investigate the time-resolved resonance fluorescence (RF) of the singly charged exciton (trion) and determine an Auger recombination rate $\gamma_a = 2.3\ \mu s^{-1}$. In our appropriately designed sample structure, this rate is of the same order of magnitude as the tunneling rate from the reservoir to the QD. This enables us to determine in detail how Auger recombination influences both the line width and intensity of the observed trion resonance. The experimental results are well accounted for by a rate model of the charge carrier dynamics. The model shows that a fast extrinsic process that replenishes the Auger ejected carrier can improve the optical properties, i.e., reduce the line width and increase the maximum intensity of the emitted light.

The investigated single InAs self-assembled QD is embedded in an (Al)GaAs heterostructure between a highly doped GaAs layer as a charge reservoir and a metallic top gate electrode (see Methods and Supporting Information for details). Applying a suitable voltage to the gate allows us to controllably transfer a single charge from the reservoir to the QD via tunneling.

Received: March 12, 2016
Revised: April 10, 2016
Published: April 18, 2016

DOI: 10.1021/acs.nanolett.6b01082
Nano Lett. 2016, 16, 3367−3372

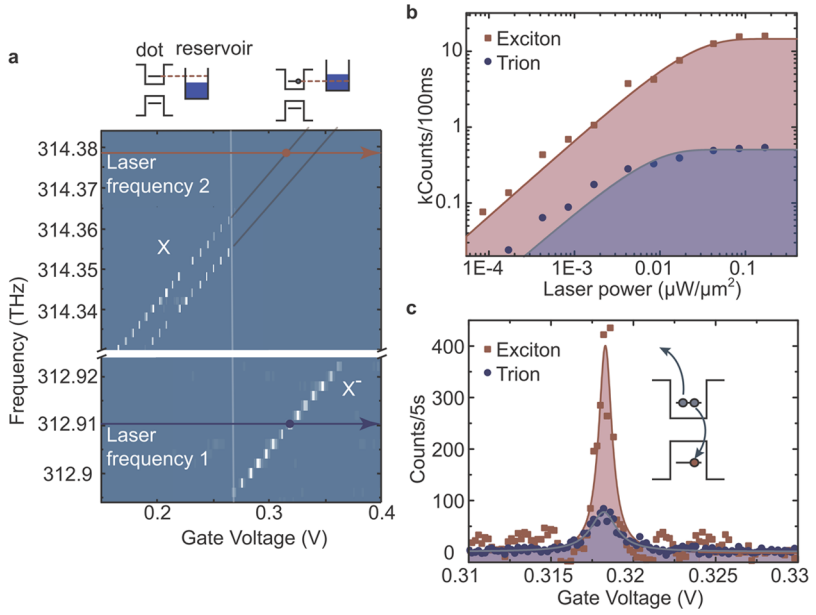

Figure 1. (a) Resonance fluorescence (RF) scan of the exciton (X) and trion (X^-) for different laser excitation energies and gate voltages. The red and blue arrows indicate the voltage scan in panel c, where we excite simultaneously on the trion (frequency 1) and exciton energy (frequency 2). The vertical white line marks the gate voltage where the Fermi energy in the charge reservoir is in resonance with the electron ground state in the dot, switching between the exciton and trion transistion. (b) Intensity of the RF signal of the trion (blue dots) and the exciton (red rectangles) for different laser excitation power. The exciton RF intensity exceeds the trion intensity by more than 1 order of magnitude. (c) Simultaneously measured RF spectra of the trion (blue dots) and the exciton (red rectangle). The observation of the exciton at this gate voltage is possible because of Auger recombination that emits the electron from the QD, leaving it in the uncharged ground state. This uncharged dot can now be excited at the exciton transition.

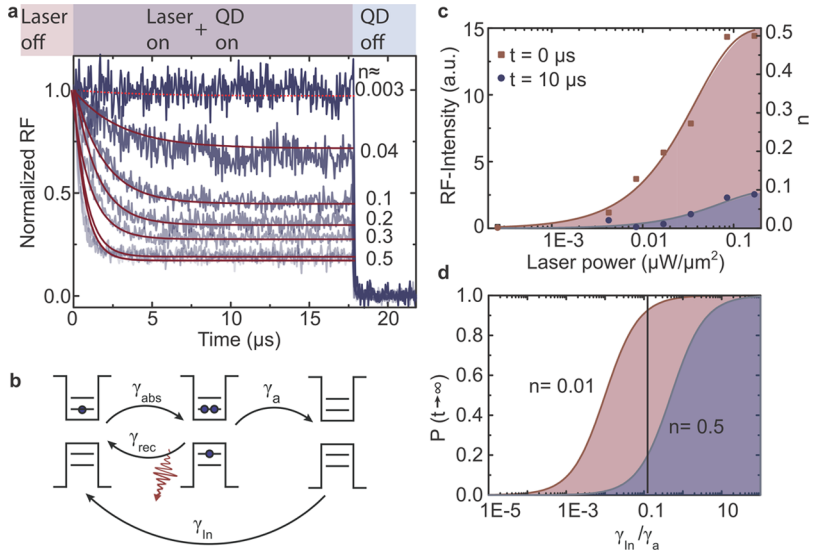

Figure 2. (a) Time-resolved RF of the trion transition. The laser is switched on at $t = 0$ with different laser excitation powers, which means with different average occupation of the dot with a charged trion n (see eq 2). Increasing the average occupation n results in a faster exponential decay and a smaller equilibrium amplitude, due to an increasing probability for an Auger recombination. (b) Schematic illustration of the different processes with rates for tunneling, γ_{In}; Auger recombination, γ_a; absorption, γ_{abs}; and recombination, γ_{rec}. (c) Intensity of the trion transition for different laser powers at $t = 0$ (red rectangles) and at $t = 10$ μs (blue dots), taken without normalization from panel a. (d) Calculations of the normalized steady-state trion RF intensity for different ratios between tunneling and Auger rate, γ_{In}/γ_a. For tunneling rates much smaller than the Auger rate, $\gamma_{In}/\gamma_a \ll 1$, the RF signal is suppressed, while $\gamma_{In}/\gamma_a \gg 1$ yields a strong signal from the trion transition. The calculations are shown for high laser excitation power (blue line) and small laser excitation power (red line).

Depending on the charging state of the dot, either the exciton transition or the trion transition is observed in RF.

In Figure 1a, the RF of the QD is shown as a function of gate voltage. Below a gate voltage of about 0.27 V, the Fermi level in the back contact is below the lowest electron state in the QD and the QD is uncharged (sketched schematically in Figure 1a, top). At $V_g = 0.27$ V, the first electron tunnels into the QD and RF of the trion transition X^- is observed around 312.9 THz. The linear shift of the resonances is caused by the gate voltage-induced Stark effect.[27]

DOI: 10.1021/acs.nanolett.6b01082
Nano Lett. 2016, 16, 3367−3372

We measure the RF intensity of the trion (blue data points in Figure 1b) and the exciton (red data points in Figure 1b) for a wide range of laser powers. The exciton RF intensity exceeds the trion intensity by more than an order of magnitude. This can be explained by an Auger process of the trion, where the nonradiative electron−hole recombination will eject the additional electron. The trion RF signal is quenched until an electron tunnels back into the QD. This reduces the integrated intensity of the trion transition. To test the assumption that the reduced intensity is caused by an Auger process, we make use of the fact that the empty dot should exhibit resonance fluorescence of the uncharged exciton. Therefore, we apply a gate voltage so that in equilibrium the dot is charged and illuminate the sample with two lasers: The first laser (frequency 1) is in resonance with the trion energy (blue dot in Figure 1a), and the second laser (frequency 2) is in resonance with the extrapolated (nonequilibrium) exciton energy (red dot in Figure 1a). The spectrally resolved intensities of the exciton and the trion transition under two-laser excitation are shown in Figure 1c. We observe both the resonance fluorescence of the exciton and the trion at the same gate voltage $V_g = 0.318$ V (for more details, see Supporting Information). At this gate voltage, the QD is charged with a single electron in equilibrium, and no resonance fluorescence of the exciton transition is observed for single laser excitation (see Figure 1a). Under two-laser illumination, the excitation of the trion together with the Auger recombination will result in an empty dot; see inset in Figure 1c. This nonequilibrium situation enables RF of the exciton transition until an electron tunnels back into the dot from the charge reservoir. The intensity of the exciton (red data points) exceeds the intensity of the trion (blue data points) by a factor of 5 in Figure 1c. The lower intensity of the trion compared to the exciton indicates that the Auger recombination rate, γ_a, is higher than the tunneling rate, γ_{In}, so that the dot is predominantly empty, i.e., in the nonequilibrium situation (further support for Auger recombination as the underlying mechanism is discussed in the Supporting Information).

In the following, we will determine the Auger recombination rate in a time-resolved m-shot RF measurement with $m = 5 \times 10^5 - 10^7$ and a repetition rate of 20 ms^{-1}. The laser energy is adjusted so that a RF signal will occur at the trion transition. For each shot, we first prepare a singly charged QD (see schematic in Figure 2b, left) by setting the gate voltage to $V_g = 0.318$ V and turning the laser illumination off for 25 μs. At $t = 0$, the laser is switched on and the QD can be excited in the trion state with the absorption rate γ_{abs}, see Figure 2b, middle (see Supporting Information for details about background correction). When the charged QD is in the excited state X^-, Auger recombination can occur with a rate γ_a. The resulting electron emission switches the trion resonance off (see Figure 2b, right) until an electron tunnels from the reservoir back into the dot. The evolution from a QD that is charged with 100% probability (at $t = 0$) to a steady-state situation, where the intensity is given by the competition between Auger emission and tunneling, is observed as an exponential decay with the relaxation rate γ_m. Figure 2a displays the corresponding signals for seven representative laser excitation powers, which determine the absorption rate γ_{abs} and hence the probability n for a trion inside the QD. The latter corresponds to the probability for the occupation of the upper level in a two-level system.[28,29] The conversion from laser power to n is given by the saturation curve of the QD (red curve and data points in Figure 2c, see below). Note that in Figure 2a the RF signal at $t = 0$ is normalized; the absolute intensity for $n = 0.003$ is much smaller than for $n = 0.5$. For $n = 0.003$ (low laser power), the time evolution of the normalized RF signal is nearly constant because the dot is predominantly in the singly charged state (Figure 2 b, left). As a consequence, the Auger recombination is negligible. With increasing n, the decrease in the RF signal becomes more pronounced. For example, for $n = 0.1$, the normalized signal drops to a steady-state value of 0.5. At this laser excitation power, 50% of the measurements end in the situation where the electron was removed from the QD, due to the Auger recombination. For saturated excitation ($n = 0.5$), the RF is reduced by 80% in the steady state. As sketched in Figure 2b, this signal quench depends on both the Auger recombination rate γ_a and the tunneling rate γ_{In}. While the former is difficult to influence, the latter is tunable by the thickness of the tunneling barrier.

How the drop in the RF signal depends on these two parameters can be determined by a model based on rate equations. The time evolution of the normalized RF signal is given by the differential equation

$$\dot{P}_f(t) = \gamma_{In} P_{nf}(t) - n\gamma_a P_f(t) \tag{1}$$

where P_{nf} and P_f are the occupation probabilities for the empty dot (nonfluorescent state) and the charged dot (fluorescent state), respectively.

The dependence of the upper state population, n, on the excitation power, p, is given by the saturation curve[28,29]

$$n(\Omega, \Delta\omega) = \frac{1}{2} \frac{\Omega^2 T_1/T_2}{\Delta\omega^2 + T_2^{-2} + \Omega^2 T_1/T_2} \tag{2}$$

with the diagonal and off-diagonal damping constants T_1 and T_2, the Rabi frequency $\Omega \propto \sqrt{p}$, and the detuning $\Delta\omega$ ($\Delta\omega = 0$ in Figure 2).

The initial condition $P_f(0) = 1$ is used to solve eq 1. We obtain

$$P_f(t) = \frac{\gamma_{In} + n\gamma_a e^{-\gamma_m t}}{\gamma_{In} + n\gamma_a} \tag{3}$$

$P_f(t)$ directly reflects the measured transients in Figure 2a with γ_m given by

$$\gamma_m = \gamma_{In} + n\gamma_a \tag{4}$$

To determine the Auger recombination rate, we use the tunneling rate $\gamma_{In} = 0.2$ μs^{-1}, derived from pulsed measurements of the excitonic RF (see Supporting Information and ref 30). Using a fit of eq 3 to the data in Figure 2a with the appropriate values of n (red lines), an Auger recombination rate $\gamma_a = 2.3$ μs^{-1} is obtained. This value is orders of magnitude smaller than Auger rates found in colloidal QDs. For example, $\gamma_a = 0.1$ ps^{-1} for CdSe dots of size $a = 2$ nm.[11] The discrepancy can be explained by a pronounced size dependence of the Auger rate, which was calculated[20] to scale as $a^{-6.5}$. Other properties such as the bandgap or details of the electronic structure play only a minor role for the Auger recombination rate in quantum dots.[31,32] The radius is not clearly defined for self-assembled QDs, which are much stronger confined in the growth direction (z) than in the lateral directions (x, y). Using the above scaling law and the measured Auger rate of 2.3 μs^{-1}, we derive an effective radius of $a = 10$ nm. This is in reasonable agreement with the typical dimensions of self-assembled QDs, $a_x \approx a_y \approx 10$ nm and $a_z \approx 3$ nm. Note that the relaxation rate

DOI: 10.1021/acs.nanolett.6b01082
Nano Lett. 2016, 16, 3367−3372

γ_m is given by both Auger and tunneling rates. More importantly, a significant drop in the RF intensity can be observed only when the tunneling rate is similar to or smaller than the Auger recombination rate. Otherwise, an Auger ejected electron will be replaced instantaneously from the reservoir. Figure 2d shows a calculation of the RF intensity in the steady state, $t \rightarrow \infty$, derived from eq 3:

$$P_f(\infty) = \frac{\gamma_{In}}{\gamma_{In} + n\gamma_a} = \frac{\gamma_{In}}{\gamma_m} \quad (5)$$

Here, two limiting cases are displayed, corresponding to weak excitation $n = 0.01$ (red line) and saturation $n = 0.5$ (blue line). The influence of the tunneling rate on the trion RF intensity is clearly visible. For high tunneling rates $\gamma_{In} > 100\gamma_a$, the RF intensity is unaffected by Auger processes. This is the regime where most experiments have been performed on self-assembled QDs. In the opposite regime, $\gamma_{In} < 0.001\gamma_a$, which applies to colloidal QDs, Auger processes have a strong influence on the optical properties and, for RF measurements, the intensity is completely quenched. In the present sample, a thick tunneling barrier was chosen; therefore, we are in the intermediate range, $\gamma_{In} \approx \gamma_a$. Here, the RF intensity is affected by the laser power, which changes the normalized RF signal between 0.2 and ≈1 (see vertical line in Figure 2d).

In the following, we use a time-resolved two-color m-shot RF measurement to substantiate that the Auger processes indeed ejects an electron, leading to an empty QD, and that equilibrium will be reestablished by tunneling. As shown in Figure 3, we first excite the QD in resonance with the trion

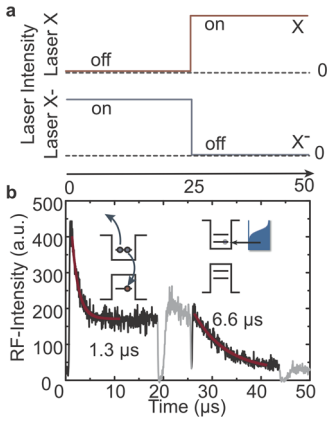

Figure 3. (a) Schematic picture of the laser pulse sequence for the two-color time-resolved measurement of the Auger recombination and tunneling rate. (b) The measurement shows an exponential decay of the RF trion signal, after switching on the first laser labeled with X^- at $t = 0$, due to the Auger recombination. Switching on the second laser, to resonant excite the exciton for $t > 25$ μs, yields a second exponential decay due to tunneling of an electron into the QD. The gray data points are used for background correction (see Supporting Information).

transition until a steady state is obtained (see also Figure 2a). Then the excitation frequency is changed to the exciton using a second laser. As seen in Figure 3b, an RF signal of the exciton is observed after switching the laser frequencies at $t = 25$ μs. This clearly shows that there is a nonvanishing probability of finding the QD in an empty state after RF excitation of the trion.

For $t > 25$ μs, an exponential decay in the exciton signal is observed with a relaxation rate of about $\gamma_r = 0.15$ μs^{-1}. The good agreement of this value with the tunneling rate $\gamma_{In} = 0.2$ μs^{-1}, obtained from pulsed gate voltage measurements (see Supporting Information), strongly supports our assumption that the dot is recharged by tunneling. The small discrepancy between γ_r and γ_{In} can be explained by optical blocking under RF excitation.[30]

The interplay between electron tunneling and Auger recombination not only has a strong influence on the intensity of the trion resonance but also affects its line width. Figure 4a shows the time-dependent trion RF resonance from $t = 0$ (initialization, singly charged QD) to $t = 3$ μs (charging state dependent on the interplay between Auger and tunneling processes). The data was recorded by measuring the time-dependent RF for different detuning $\Delta\omega$ between the laser and the trion resonance, as shown in Figure 4b. Figure 4c displays two normalized spectra, taken at $t = 0$ and $t = 10$ μs, together with the corresponding Lorentzian fits. Clearly, the line width is increasing with increasing time, as also summarized in Figure 4d. For very short times, we observe a line width of 1.3 μeV, while for a steady-state situation ($t \rightarrow \infty$) the resonance is a factor of 1.6 broader.

This broadening can directly be explained by the influence of the detuning on the relaxation rate, γ_m, which in turn depends on the trion population, n, see eq 4. Equation 2 shows that n decreases with increasing laser detuning, $\Delta\omega$, and this leads to a reduced relaxation rate, γ_m, and a reduced probability for Auger recombination. The measured relaxation rate, evaluated from fits to the transients in Figure 4b, is summarized in Figure 4e for different detunings, $\Delta\omega$. The data can be described well by eqs 2 and 4, see blue solid line in Figure 4e. We observe a strongly reduced relaxation rate, γ_m, at the edges of the transition compared to the center of the resonance.

The line width of the trion transition without an Auger process already depends on the laser excitation power, via the so-called power broadening. This line width follows from

$$w(t = 0) = \frac{2}{T_2}\sqrt{1 + \Omega^2 T_1 T_2} \quad (6)$$

where the Rabi-frequency, Ω, is given by the excitation power.[33] We performed the measurement shown in Figure 4a for different laser excitation powers and determined the line width of the trion resonance at $t = 0$ and $t = 10$ μs. The measured line width of the transition at $t = 0$ is shown as red data points in Figure 4f together with a fit of eq 6 to the data (red line in Figure 4f). The line width of the trion transition at $t = 10$ μs can then be calculated without any adjustable parameter, using eqs 2, 5, and 6 for $t \rightarrow \infty$:

$$w(t \rightarrow \infty) = \frac{1}{T_2}\sqrt{\frac{T_2^2 w(t = 0)^2(\gamma_a + 2\gamma_{In}) - 4\gamma_a}{2\gamma_{In}}} \quad (7)$$

It is plotted in Figure 4f as a blue line and is in good agreement with the measured data. The T_2 time can be determined from the line width at $t = 0$ for small laser excitation power to be $T_2 = 975$ ps, in agreement with previous estimates.[28]

Our study allows the following conclusions: (i) Auger recombination leads to not only a reduced intensity but also an increased line width. (ii) To improve both, the required time to replenish the ejected carrier should be shorter than the Auger recombination time. This can easily be achieved in self-assembled QDs, e.g., by tunneling from a charge reservoir; however, it may be challenging for small colloidal dots having

DOI: 10.1021/acs.nanolett.6b01082
Nano Lett. 2016, 16, 3367−3372

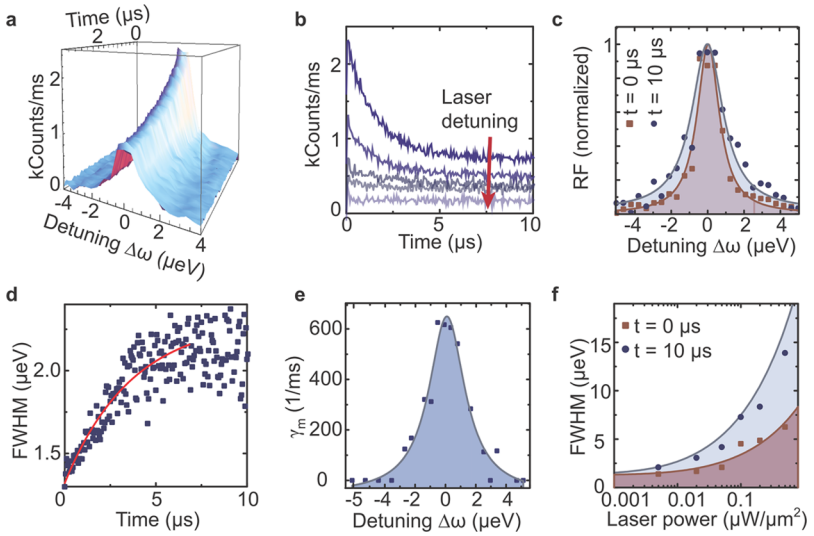

Figure 4. (a) Time-resolved measurement of the trion line after switching on the resonant excitation at $t = 0$ with a laser power of about $0.05\frac{\mu W}{\mu m^2}$. For increasing time duration, the line gets broadened and the maximum intensity is quenched by 60%. (b) The time-evolution of the line shapes in panel a has been determined by evaluation of transients for different laser detuning, showing different time constants for the relaxation rate, γ_m. (c) Normalized trion resonance at $t = 0$ (red) and at $t = 10$ μs (blue). (d) The line width of the trion transition increases from 1.3 μeV by a factor of 1.6 up to about 2.2 μeV. (e) The relaxation rate, γ_m, is plotted versus the laser detuning. We observe a decreasing relaxation rate for increasing detuning of the laser from the resonance maximum. (f) Line width of the trion transition at $t = 0$ (red) and at $t = 10$ μs (blue) for different laser excitation powers. The red line is a fit to the data, and the blue line is calculated by the rate equation model (see main text).

picosecond Auger recombination times. (iii) The Auger-induced broadening can be circumvented by measurements faster than the Auger recombination time.

In summary, we have studied the Auger recombination in a single self-assembled QD using time-resolved resonance fluorescence measurements. Our findings show that in samples that are only weakly coupled to a charge reservoir, the Auger process has a strong influence on the line shape of the trion transition: The line width increases and the maximum intensity decreases. Using time-resolved RF and two-color excitation, we were able to determine both the tunneling rate and the Auger recombination rate, a quantity that was not well-known for self-assembled dots. Furthermore, we have modeled the carrier dynamics in the QD using a simple rate equation which includes radiative recombination, Auger processes, and tunneling. The calculations are in good agreement with our measurements and show that a fast tunneling time improves the optical properties of the QD.

Methods. The investigated sample was grown by molecular beam epitaxy (MBE) and resembles a field-effect-transistor structure,[34,35] containing a layer of self-assembled InAs QDs. In detail, a 300 nm GaAs layer was deposited on a semi-insulating GaAs substrate, followed by a 50 nm heavily silicon-doped GaAs layer, which forms a nearly metallic back electrode and electron reservoir. A tunneling barrier, consisting of 15 nm GaAs, 10 nm $Al_{0.34}Ga_{0.66}As$, and 5 nm GaAs, was grown, which separates the InAs QDs from the doped back contact. The InAs QDs are formed by growing 1.6 monolayers of InAs partially capped by 2.7 nm GaAs and flushed at 600 °C for 1 min to shift the emission wavelength to ≈950 nm. They are further capped by a 27.5 nm GaAs layer, a 140 nm super lattice (35 periods of 3 nm AlAs and 1 nm GaAs) and 10 nm GaAs. The ohmic back contact is formed by AuGe and Ni evaporation and annealing (see Supporting Information for more details of the sample). Transparent Schottky gates are prepared on the sample surface by standard optical lithography and deposition of 7 nm NiCr. On top of these gates, a zirconium solid immersion lens (SIL) is mounted to improve the collection efficiency of the QD emission.[36] A gate voltage applied between the top gate and the Ohmic back contact induces an external electric field and controls the charge state in the QD.[37]

We use a confocal microscope setup in a bath-cryostat at a temperature of 4.2 K. For the RF measurements, the exciton (X) or trion (X^-) transitions are driven resonantly by a linearly polarized and frequency stabilized tunable diode laser. In a confocal geometry, both laser excitation and QD emission are guided along the same path, using a 10:90 beam splitter. Single QD resolution is archived by a 0.65 NA objective lens in front of the above-mentioned SIL, giving a spot size of 1 μm. The emission of the QD is collected behind a polarizer (Thorlabs LBVIS050-MP with an extinction ration of 10^7), which is polarized orthogonally to the excitation laser and suppresses the laser light by a factor of 10^7. The RF signal of the QD is detected by an avalanche photo diode (APD) and is recorded using a time-to-digital converter with a time resolution of 81 ps.

■ ASSOCIATED CONTENT

Supporting Information

The Supporting Information is available free of charge on the ACS Publications website at DOI: 10.1021/acs.nanolett.6b01082.

Measurement details and measurements of the tunneling rates (PDF)

■ AUTHOR INFORMATION

Corresponding Author

*E-mail: annika.kurzmann@uni-due.de.

Notes

The authors declare no competing financial interest.

DOI: 10.1021/acs.nanolett.6b01082
Nano Lett. 2016, 16, 3367−3372

■ ACKNOWLEDGMENTS

A.L. and A.D.W. gratefully acknowledge support of BMBF - Q.com-H 16KIS0109 and the DFH/UFA CDFA-05-06

■ REFERENCES

(1) Bimberg, D.; Grundmann, M.; *Ledentsov Quantum Dot Heterostructures*; Wiley: New York, 1999.
(2) Klimov, V. I. *Nanocrystal Quantum Dots*, 2nd ed.; CRC Press: Boca Raton, FL, 2010.
(3) Braam, D.; Mölleken, A.; Prinz, G. M.; Notthoff, C.; Geller, M.; Lorke, A. *Phys. Rev. B: Condens. Matter Mater. Phys.* **2013**, *88*, 125302.
(4) Kuhlmann, A. V.; Houel, J.; Ludwig, A.; Greuter, L.; Reuter, D.; Wieck, A. D.; Poggio, M.; Warburton, R. J. *Nat. Phys.* **2013**, *9*, 570−575.
(5) Houel, J.; Kuhlmann, A. V.; Greuter, L.; Xue, F.; Poggio, M.; Gerardot, B. D.; Dalgarno, P. A.; Badolato, A.; Petroff, P. M.; Ludwig, A.; Reuter, D.; Wieck, A. D.; Warburton, R. J. *Phys. Rev. Lett.* **2012**, *108*, 107401.
(6) Jha, P. P.; Guyot-Sionnest, P. *ACS Nano* **2009**, *3*, 1011−1015.
(7) Park, Y.-S.; Bae, W. K.; Pietryga, J. M.; Klimov, V. I. *ACS Nano* **2014**, *8*, 7288−7296.
(8) Cohn, A. W.; Rinehart, J. D.; Schimpf, A. M.; Weaver, A. L.; Gamelin, D. R. *Nano Lett.* **2014**, *14*, 353−358.
(9) Klimov, V. I.; Mikhailovsky, A. A.; Xu, S.; Malko, A.; Hollingsworth, J. A.; Leatherdale, C. A.; Eisler, H.-J.; Bawendi, M. G. *Science* **2000**, *290*, 314−317.
(10) Efros, A. L.; Rosen, M. *Phys. Rev. Lett.* **1997**, *78*, 1110−1113.
(11) Klimov, V. I.; Mikhailovsky, A. A.; McBranch, D. W.; Leatherdale, C. A.; Bawendi, M. G. *Science* **2000**, *287*, 1011−1013.
(12) Caruge, M.; Halpert, J. E.; Wood, V.; Bulovic, V.; Bawendi, M. G. *Nat. Photonics* **2008**, *2*, 247−250.
(13) Cho, K.-S.; Lee, E. K.; Joo, W.-J.; Jang, E.; Kim, T.-H.; Lee, S. J.; Kwon, S.-J.; Han, J. Y.; Kim, B.-K.; Choi, B. L.; Kim, J. M. *Nat. Photonics* **2009**, *3*, 341−345.
(14) Brokmann, X.; Messin, G.; Desbiolles, P.; Giacobino, E.; Dahan, M.; Hermier, J. P. *New J. Phys.* **2004**, *6*, 99.
(15) Michler, P.; Imamoglu, A.; Mason, M. D.; Carson, P. J.; Strouse, G. F.; Buratto, S. K. *Nature* **2000**, *406*, 968−970.
(16) Lounis, B.; Bechtel, H. A.; Gerion, D.; Alivisatos, P.; Moerner, W. E. *Chem. Phys. Lett.* **2000**, *329*, 399−404.
(17) Park, Y. S.; Bae, W. K.; Padilha, L. A.; Pietryga, J. M.; Klimov, V. I. *Nano Lett.* **2014**, *14*, 396−402.
(18) Bae, W. K.; Park, Y. S.; Lim, J.; Lee, D.; Padilha, L. A.; McDaniel, H.; Robel, I.; Lee, C.; Pietryga, J. M.; Klimov, V. I. *Nat. Commun.* **2013**, *4*, 2661.
(19) Turk, M. E.; Vora, P. M.; Fafarman, Q. T.; Diroll, B. T.; Murray, C. B.; Kagan, C. R.; Kikkawa, J. M. *ACS Nano* **2015**, *9*, 1440−1447.
(20) Vaxenburg, R.; Rodina, A.; Shabaev, A.; Lifshitz, E.; Efros, A. L. *Nano Lett.* **2015**, *15*, 2092−2098.
(21) Michler, P.; Kiraz, A.; Becher, C.; Schoenfeld, W.; Petroff, P.; Zhang, L.; Hu, E.; Imamoglu, A. *Science* **2000**, *290*, 2282−2285.
(22) Yuan, Z.; Kardynal, B. E.; Stevenson, R. M.; Shields, A. J.; Lobo, C. J.; Cooper, K.; Beattie, N. S.; Ritchie, D. A.; Pepper, M. *Science* **2002**, *295*, 102−105.
(23) Kuhn, A.; Hennrich, M.; Rempe, G. *Phys. Rev. Lett.* **2002**, *89*, 067901.
(24) Kuhlmann, A. V.; Prechtel, J.; Houel, J.; Ludwig, A.; Reuter, D.; Wieck, A. D.; Warburton, R. J. *Nat. Commun.* **2015**, *6*, 8204.
(25) Santori, C.; Fattal, D.; Vuckovic, J.; Solomon, G. S.; Yamamoto, Y. *Nature* **2002**, *419*, 594−597.
(26) Matthiesen, C.; Geller, M.; Schulte, C. H. H.; Le Gall, C.; Hansom, J.; Li, Z.; Hugues, M.; Clarke, E.; Atatüre, M. *Nat. Commun.* **2013**, *4*, 1600.
(27) Empedocles, S. A.; Bawendi, M. G. *Science* **1997**, *278*, 2114−2117.
(28) Muller, A.; Flagg, E. B.; Bianucci, P.; Wang, X. Y.; Deppe, D. G.; Ma, W.; Zhang, J.; Salamo, G. J.; Xiao, M.; Shih, C. K. *Phys. Rev. Lett.* **2007**, *99*, 187402.
(29) Grynberg, G.; Aspect, A.; Fabre, C. *Introduction to Quantum Optics*; Cambridge University Press: New York, 2010.
(30) Kurzmann, A.; Merkel, B.; Labud, P. A.; Ludwig, A.; Wieck, A. D.; Lorke, A.; Geller, M. 2015, arXiv:1505.07682 [cond-mat.mes-hall].
(31) Pietryga, J. M.; Zhuravlev, K. K.; Whitehead, M.; Klimov, V. I.; Schaller, R. D. *Phys. Rev. Lett.* **2008**, *101*, 217401.
(32) Robel, I.; Gresback, R.; Kortshagen, U.; Schaller, R. D.; Klimov, V. I. *Phys. Rev. Lett.* **2009**, *102*, 177404.
(33) Loudon, R.; *The Quantum Theory of Light*; Oxford University Press: New York, 2010.
(34) Petroff, P. M.; Lorke, A.; Imamoglu, A. *Phys. Today* **2001**, *54*, 46.
(35) Warburton, R.; Miller, B.; Dürr, C.; Bodefeld, C.; Karrai, K.; Kotthaus, J.; Medeiros-Ribeiro, G.; Petroff, P.; Huant, S. *Phys. Rev. B: Condens. Matter Mater. Phys.* **1998**, *58*, 16221.
(36) Gerardot, B. D.; Seidl, S.; Dalgarno, P. A.; Warburton, R. J.; Kroner, M.; Karrai, K.; Badolato, A.; Petroff, P. M. *Appl. Phys. Lett.* **2007**, *90*, 221106.
(37) Drexler, H.; Leonard, D.; Hansen, W.; Kotthaus, J. P.; Petroff, P. M. *Phys. Rev. Lett.* **1994**, *73*, 2252.

DOI: 10.1021/acs.nanolett.6b01082
Nano Lett. 2016, 16, 3367−3372